Analysis of Wave Propagation Models With Radio Network Planning Using Dual Polarized MIMO Antenna for 5G Base Station Applications

ANUDEEP BELLARY[1], **(Student Member, IEEE),**
KRISHNAMOORTHY KANDASAMY[1], **(Member, IEEE),**
AND PATNAM HANUMANTHA RAO[2], **(Senior Member, IEEE)**

[1]Department of ECE, National Institute of Technology Karnataka, Surathkal, Mangalore 575025, India
[2]Microwave Communication and Antenna Division, SAMEER-Centre for Electromagnetics, Chennai 600113, India

Corresponding author: Anudeep Bellary (deepubellary30@gmail.com)

ABSTRACT Dual polarized printed multiple input multiple output (MIMO) antenna for Band 42 (3.4 - 3.6 GHz) with wave propagation models is presented. Polarization and spatial diversity are achieved by utilizing two printed bow-tie antennas in orthogonal orientation. The designed dual polarized antenna element with 2×2, 4×4 and 8×8 massive MIMO antenna configuration radiation patterns are deployed in selected geographical situation for detailed radio network planning using FEKO-WinProp platform. Knife edge diffraction, extended walfisch-ikegami and dominant path wave propagation models are implemented with designed MIMO antenna configurations. Modulation schemes of QPSK and QAM with corresponding data rates and throughput for all propagation models are presented. The signal strength and quality reflecting parameters reference signal received power (RSRP), received signal strength indicator (RSSI), reference signal received quality (RSRQ), and signal to noise plus interference ratio (SNIR) are also evaluated for each model. From the simulation results dominant path model provides data rate and throughput of 3.827, 995 MBit/s and 3.577, 930.1 MBit/s for single stream of data in uplink and downlink respectively. The maximum data rate of 1.37 GBits/s is achieved for deployed base stations with 8×8 massive MIMO antenna configuration effectively covering the entire geographical site.

INDEX TERMS Dual polarization, 5G, MIMO, radio network planning, wave propagation models.

I. INTRODUCTION

Basestation antennas gained a lot of attention over the past few decades with various types of antennas and with different structures [1]–[3]. Mainly antennas include patch antennas [4], [5] slot antennas [6], cross dipole antennas [7]–[9], with polarization diversity technique by utilizing different polarization became popular for base station antenna. Compact Dual polarized antennas are selected for base station antennas for their interesting features to overcome multipath fading and increasing channel capacity [10]–[15]. The ability of increasing channel capacity and combating the effect of multipath fading effect with polarization diversity received utmost attention in designing base station antennas [16]. The current development of 5G networks, focusing

The associate editor coordinating the review of this manuscript and approving it for publication was Shah Nawaz Burokur.

on the possibility to multiplex data streams parallely with time or frequency resource through multiple input multiple output (MIMO) antenna systems.

From analog communications to the existing long term evolution (LTE) new technology has evolved comprising of new standard. Antenna technology also advancing starting from monopoles to present complex massive MIMO antennas [17]. To sustain the demand of network capacity the requirement of new technologies with next level set of standards are needed namely 5G [18]. 3rd generation partnership project (3GPP) also focusing and standardizing the requirements for 5G [19]. The current scenario for telecom operators is to maintain multi-standard networks by expanding the already existing 4G (fourth generation) long term evolution (LTE) and gradually moving towards new technology generations [20]. Simultaneously the network operators are maximizing their LTE network by applying

LTE-Advanced for providing capacity scalability and also to make it flexible to adopt cellular connectivity. Recently, the mobile traffic increased drastically (also by changes induced by COVID-19) which allows antennas to further optimize towards 6G systems [21]. For 5G systems to be reliable RF propagation models have to be generated to ensure standard performance which also includes path loss models [22], [23]. To meet these requirements of users with high connectivity and data rates, 5G deployment has to accommodate huge data traffic and unlock the connectivity issues.

In this paper, compact dual polarized MIMO antenna operating in Band 42 with wave propagation models for 5G applications is presented. The proposed antenna configuration is miniaturized and provides high isolation of 32 dB with stable radiation patterns and an average gain of 8.26 dB for entire band of operation. To the best of the author's knowledge the detailed radio network planning along with wave propagation models for the designed antenna using FEKO Winprop platform so far has not been reported. The designed antenna element with 2×2, 4×4 and 8×8 MIMO antenna configuration radiation patterns are deployed in practical scenario for complete network planning with different wireless standards to support 5G requirements. The analysis of deployed base stations with modulation schemes of QPSK and QAM for all wave propagation models are also discussed. The signal strength and quality reflecting parameters RSRP, RSRQ, RSSI and SNIR are analyzed with each propagation model for selected geographical site.

II. DUAL POLARIZED MIMO ANTENNA
A. ANTENNA DESIGN DETAILS
The geometry and development of the proposed dual polarized antenna(DPA) are shown in Fig. 1. The antenna contains three layers radiator, printed feed structure and a PEC reflector. The main radiator of the proposed antenna consists of two printed dipoles in orthogonal orientation and fabricated on FR4 substrate with relative dielectric constant of 4.4. The orthogonal arrangement of two such dipole antennas in cross-pairs provides two different polarized radiation patterns. To obtain better isolation, two pairs of L-slots are etched on each arm of the radiator. In addition to L-slots, U notches are created between two adjacent arms of the antenna as shown in Fig. 1. The proposed shape of the each arm with L shaped slots and U-notches on the edges of the radiator enhance the port to

port isolation and also supress the cross polarization between antenna elements.

The feed structure is printed on two vertical substrates with Γ shaped feed lines, which are properly designed for good impedance matching on FR4 substrate as shown in Fig. 2. The bottom PEC reflector contains the extended feed lines of the two vertical substrates where the two 50Ω coaxial cables for the feed structures are connected. It is observed that the two individual ports of dual polarized antennas with this arrangement provide better port to port isolation. Optimizations are performed using FEM based 3D electromagnetic (EM) simulation software Ansoft HFSS 19.0. The geometric parameters for the proposed dual polarized antenna element are tabulated in Table 1.
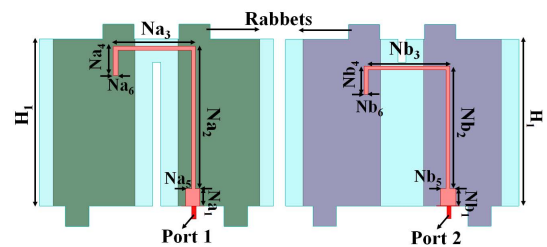

FIGURE 2. Geometry of the proposed feed network.

TABLE 1. Optimized dimensions of the proposed dual polarized MIMO antenna.

Parameters	Values (mm)	Parameters	Values (mm)
L1	40	L2	13
L3	7.5	L4	7
L5	4.5	L6	4
W1	0.5	D1	5.6
H1	21.42	Na1	2.1
Na2	18.2	Na3	10.5
Na4	3.7	Na5	1.8
Na6,Nb6	0.5	Nb1	2.1
Nb2	15.7	Nb3	11
Nb4	3.6	Nb5	2

B. SIMULATED AND MEASURED RESULTS
Simulated and measured S-Parameters for the dual polarized antenna element are shown in Fig. 3. From the measured results it is observed with a VSWR of < 1.5 and high isolation of 32 dB are achieved for entire band of interest. The measured gain and efficiency measurement by utilizing Q method are calculated for both the polarized antenna elements as shown in Fig. 4. An average gain of 8.26 dB is obtained for each single dual polarized antenna element. The fabricated prototype of the proposed dual polarized MIMO antenna element are shown in Fig. 5(a) and (b).
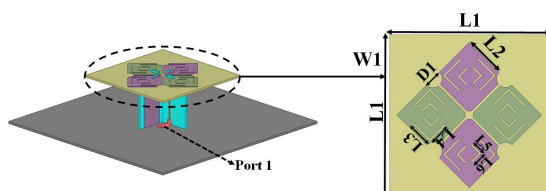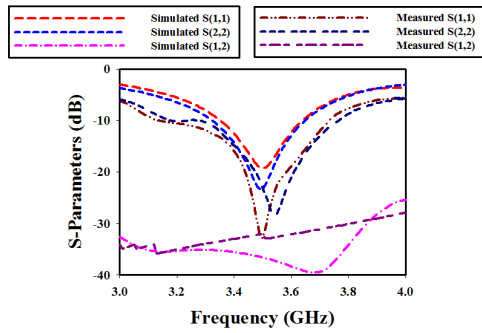

FIGURE 1. Geometry of the proposed DPA.

FIGURE 3. Simulated and measured S-parameters of the proposed DPA.
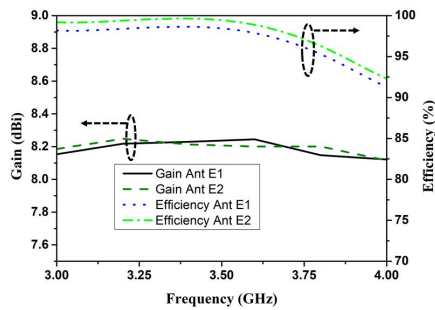

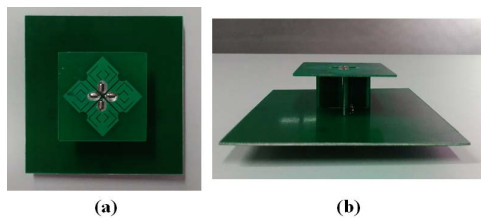**FIGURE 4.** Measured gain and efficiency of the proposed DPA.

FIGURE 5. Fabricated prototype of proposed DPA (a) Top view and (b) Side view.

The measured and simulated radiation patterns at different frequencies of 3.4 GHz, 3.5 GHz and 3.6 GHz for dual polarized MIMO antenna element in both E and H planes when antenna port 1 is excited are shown in Fig. 6(a), Fig. 6(b) and Fig. 6(c) respectively. From the measured results cross polarization levels are below -25 dB in both azimuth and elevation planes with front-to-back ratio of 30 dB. The difference in measured and simulated results may be attributed to the measurement and fabrication errors. The far field measurement setup for the proposed dual polarized MIMO antenna element is shown in Fig. 7. The MIMO performance parameters like envelope correlation coefficient(ECC) and diversity gain(DG) are also calculated by using S-parameters for 1×2 MIMO configuration with elements E1 and E2 as shown in Fig. 8. The performance comparison of the proposed antenna with previous work is given in Table 2.
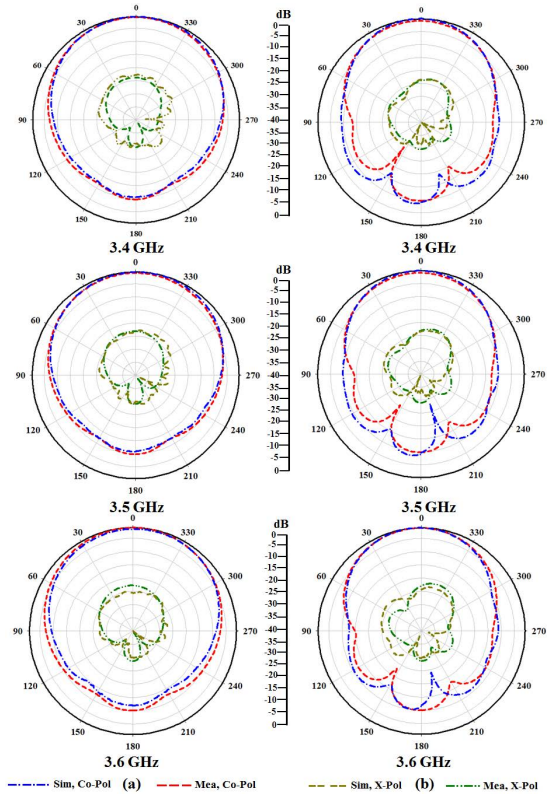

FIGURE 6. Simulated and measured radiation patterns when antenna port 1 is excited (a) E-Plane (b) H-Plane.
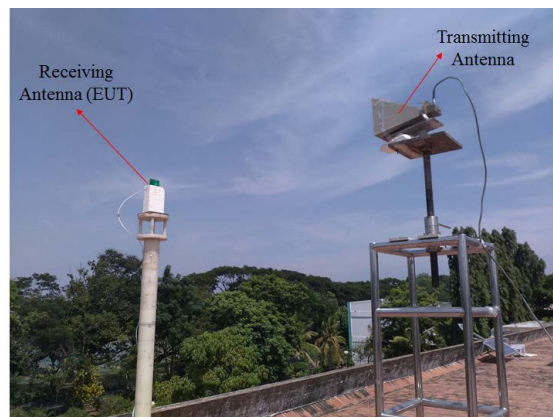

FIGURE 7. Far field measurement setup of fabricated DPA.

III. RADIO NETWORK PLANNING FOR 5G MIMO ANTENNA

A. DEPLOYMENT OF 5G MIMO ANTENNA ELEMENT

The proposed dual polarized 5G MIMO antenna is deployed in practical scenarios with different air interface wireless standards by using FEKO-WinProp software. FEKO Win-Prop 3D EM software package is utilized for simulating the model as it supports ray tracing models with 3D visualization of actual deployment in campus environment. Full 3D visualization of the environment for the antenna deployment could
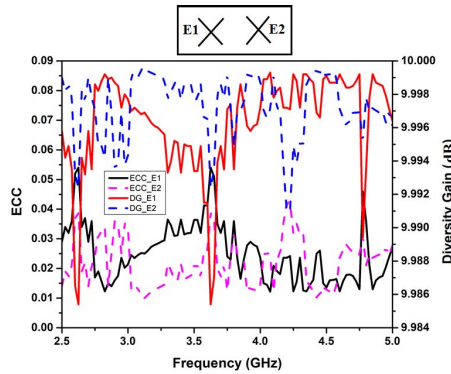
FIGURE 8. MIMO performance analysis using ECC and DG parameters.

TABLE 2. Performance comparison of proposed MIMO antenna element with previous work.

Ref.	Oper. band(GHz)	R S (λ_0)	H(λ_0)	Iso.	G
[10]	1.7 - 2.9 (52%)	0.58×0.58	0.26	26.3	8
[11]	3.3 - 3.7 (11.4%)	0.33 × 0.33	0.21	30	7
[12]	3.2 - 3.9 (19.7%)	0.36 × 0.36	0.16	40	6.8
[13]	2.45 - 2.8 (13.46%)	0.37 × 0.37	0.14	25	8.8
[14]	3.02 - 4.02 (33%)	0.5 × 0.5	0.125	25	7.9
Pro.	3.2-3.7 (14.2%)	0.46×0.46	0.25	32	8.26

not be implemented in MATLAB/ADS and it's not under the scope of the proposed work in the manuscript. Effect of various parameters like reflection, refraction, scattering, path loss, line of sight are taken into account with WinProp software which also supports different wireless standards as per 3GPP requirements. The effective coverage over the selected terrain and locations for proper deployment of the antennas are also shown with suitable graphs using WinProp software.

The different wave propagation models are considered for computing the radio coverage and radio channel analysis in various scenarios from large rural to dense urban cities. The step by step procedure for deploying the proposed 5G MIMO antenna is shown in Fig. 9.The network planning modules for different air interfaces helps to compute the overall signal and interference situation by superposing the contributions from multiple deployed transmitting sites.

The ray tracing models in WinProp [24] considers all the dominant wave propagation characteristics (reflection, diffraction, and scattering) and support the analysis of 3D building knowledge representing the given surroundings. The propagation models are three dimensional by taking into account of all 3D object data. For accurate predictions of the radio coverage the dominant path model(DPM) is applied which consists of high accuracy with short computation time. For deploying the designed 5G MIMO antenna element a geographical terrain National Institute of Technology Karnataka (NITK) campus is selected as shown in Fig. 10. and the equivalent representation of the map by using WallMan is shown in Fig. 11. The designed radiation patterns for Unit
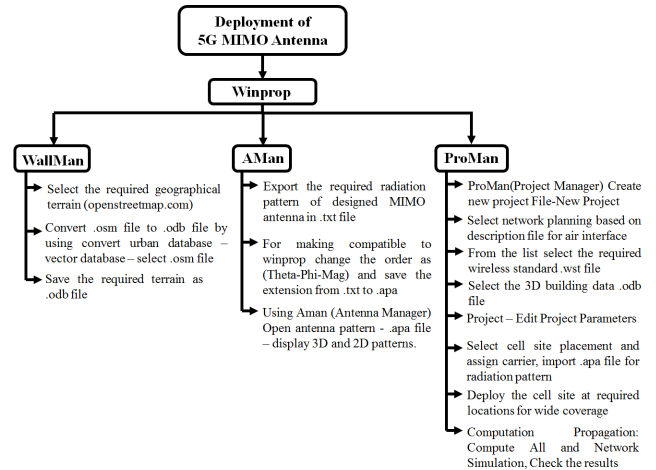

FIGURE 9. Flow chart for deployment of 5G MIMO antenna element in WinProp.

FIGURE 10. NITK campus considered locations A,B and C with respective buildings are labelled and given in map.
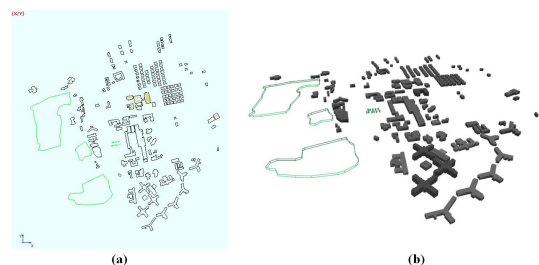

FIGURE 11. Selected geographical terrain using WallMan and ProMan (a) Layout and (b) 3D View respectively.

cell, 2 × 2, 4 × 4 and 8 × 8 massive MIMO antenna are exported from ANSYS HFSS and made compatible for WinProp by using AMAN(Antenna Manager). The obtained 3D radiation plot for MIMO antenna element is shown in Fig. 12.

The radio channel predictions in terms of time, frequency and also for the spatial domain are necessary to analyze the 5G transmission modes along with various MIMO concepts. MIMO antenna arrays are developed in different configurations on both at transmitter(Tx) and receiver(Rx) side which uses spatial multiplexing or beamforming and even
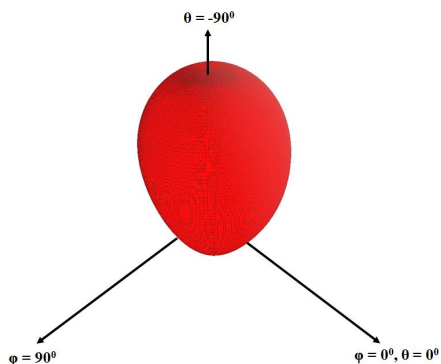
FIGURE 12. 3D Radiation pattern of Single DPA Element in AMAN.

FIGURE 13. Pictorial representation of NITK campus with deployed cell site locations.

FIGURE 14. Panoramic View from Location A focusing the east side campus. This building is marked as site 1 antenna 1 in the cell site area map.

FIGURE 15. Panoramic view from location B focusing towards building A. This building is marked as site 2 antenna 2 in the cell site area map.

FIGURE 16. Panoramic view from location C focusing the entire hostel blocks. This building is marked as site 3 antenna 3 in the cell site area map.

combination of both technologies. The signal field strength and delay with angle of depature at both Tx and Rx are considered in WinProp. This simulation tool provides several methods which are fully three dimensional by considering 3D objects data to compute all rays in 3D. The ProMan(Project Mangaer) is utilized to deploy the cell sites in selected geographical terrain and required network planning is done by using various air interfaces.

B. MEASUREMENT LOCATIONS

The measurement environment is at NITK campus and the respective deployed locations A,B and C for base station antenna are given in Fig. 10. The deployment of the MIMO antenna with different configurations can be selected to any densely populated urban areas, for convenience the campus view itself is considered and analyzed. The measurements are taken in three locations, namely at Building A (Main Academic Building) as location-A, Building B (Lecturer Hall C) as location-B and Building C(Mega Tower) as location-C which are marked on the map. Location A and location B are on two either sides of the national highway passing in between the east and west campus which are 15m apart whereas the distance between location A, location B to location C will be more than 50m. The pictorial representation of the campus with selected sites for antenna deployment are shown in Fig. 13. The panoramic views from these locations are also shown from Fig. 14 to Fig. 16. These locations were selected such that the deployed MIMO antenna sees the different environment addressing the maximum number of users.

In location A, B and C the selected MIMO antenna configurations are placed at altitude of 30m from the terrace to maintain the uniform coverage. There are other bulidings in between with various departments covering the maximum number of users. The selected three locations covers the entire campus with maximum data rate and throughput with required channel modulation schemes. The various wave propagation models are studied with different MIMO antenna configurations and analyzed.
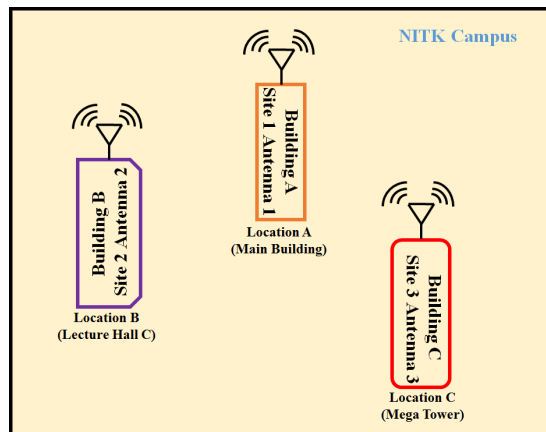
C. RADIO NETWORK PLANNING OF 5G MIMO ANTENNA

The performance of wireless communication networks depends on an efficient architecture of the network. Due to

the wide range of available air interfaces for cellular and broadcast wireless networks with their different behavior and parameter settings, radio network planning is essential to analyze the performance of the wireless network [25].

For deploying 5G, ultra-dense networks consisting of base stations with low power in suburban areas are utilized to provide high data rates. Accordingly, a fast coverage prediction model is required. Here, for 5G radio planning the dominant path model is utilized as it combines high accuracy with less computation time. The dominant path model supports wide frequency range which can be used for all types of cells with Tx antennas above, below or on the rooftop. Therefore, by considering this model the radio coverage for different air interface wireless standards are tabulated in Table 3.

TABLE 3. Radio network planning for air interface with wireless standards.

S.No	Parameters with Units	Dual Polarized Antenna Wireless Standard	
		5G TDD	5G FDD
1.	DL:Max Data Rate (MBits/s)	1.288	2.471
2.	DL:Throughput (MBits/s)	334.9	642.4
3.	UL:Max Data Rate (MBits/s)	1.378	2.643
4.	UL:Throughput (MBits/s)	358.2	687.2
5.	Received Power (dBm)	-60	-65
6.	SNIR (dB)	40	35
7.	RSRP (dBm)	-80	-85
8.	RSRQ (dB)	0	0
9.	RSSI (dBm)	-62	-64

Note: DL-Down Link, UL-Up Link.

As the 5G cellular network launching gets interconnected and utilizes the already existing 4G LTE networks. To understand the LTE(Long Term Evolution) signal strength and quality few signal type terminologies and its considerable range of values are described below [25].

- Reference Signal Received Power(RSRP) : As per 3GPP definition of RSRP is defined as the linear mean over the power contributions for the resource elements that contain cell-specific reference signals within the desired measurement frequency bandwidth. Its typical signal quality values are ≥ -80 dBm (Excellent); -80 dBm to -90 dBm (Good); -90 dBm to -100 dBm (Fair to Poor); ≤ -100 dBm (No Signal/Disconnection).

- Received Signal Strength Indicator (RSSI) : RSSI is defined as the entire received power including the desired power from the serving cell in addition to the co-channel power and other sources of noise. RSSI typical signal quality value ranges are > -65 dBm (Excellent); -65 dBm to -75 dBm (Good); -75dBm to -85 dBm (Fair); -85 dBm to -95 dBm (Poor); ≤ -95 dBm (No Signal/Disconnection)

- Reference Signal Received Quality (RSRQ) : It indicates the quality of the received reference signal. RSRQ typical signal quality value ranges are ≥ -10 dB (Excellent); -10 dB to -15 dB (Good); -15 dB to -20 dB (Fair to Poor); ≤ -20 dB (No Signal/Disconnection).

- SNIR/SNR : Signal to Noise plus Interference Ratio (A minimum of 20 dB is required to detect the RSRP/RSRQ). It indicates the throughput capacity of the channel. The typical range of values are $\geq$ 20 dBm (Excellent); 13 dBm to 20 dBm (Good); 0 dBm to 13 dBm (Fair to Poor); $\leq$ 0 dBm (No Signal/Disconnection).

WinProp platform is utilized to determine the path loss, cell coverage, signal to noise and interference ratio, throughput, maximum data rates in down link and up link, received power, individually for each transmission mode. From the tabulated data both Time division duplex(TDD) and Frequency division duplex(FDD) technologies are utilized for 5G. TDD, FDD are two different spectrum utilization techniques which are considered by mobile operators. In FDD, separate frequencies are used for uplink and downlink where as in TDD a single frequency is used for both uplink and downlink transmitting at different times.

In general, FDD is employed for better coverage, while TDD is chosen for better capacity. However, by comparing the results and range of coverage over the selected area 5G FDD standard with dual polarized antenna element consisting of three number of sites is selected. The cell site areas over the selected map is shown in Fig. 17. From the simulation results calculated path loss is observed as -80 dB at each cell site is calculated and given for cell site 1 as shown in Fig. 18. The line of sight(LOS) and non line of sight(NLOS) with respect to each cell sites are calculated and given for cell site 1 as shown in Fig. 19.
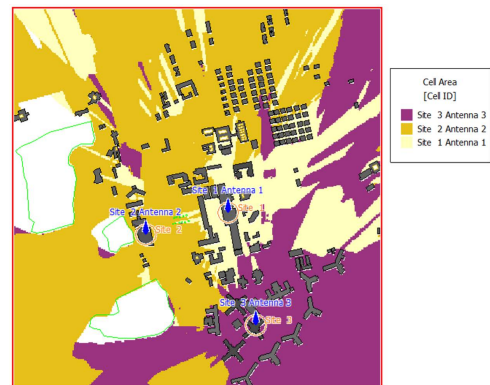

FIGURE 17. Individual cell site area in selected map.

IV. WAVE PROPAGATION MODELS FOR 5G MIMO ANTENNA

A. KNIFE EDGE DIFFRACTION MODEL

Generally, the deterministic models utilize the physical phenomena to explain the propagation of radio waves and are based on ray optical techniques. When a radio wave is considered to propagate in straight line it gets presuaded by only the present obstacles that mostly lead to reflection, diffraction and even peneration through these obstacles. But for scenarios where there is large distance between transmitter
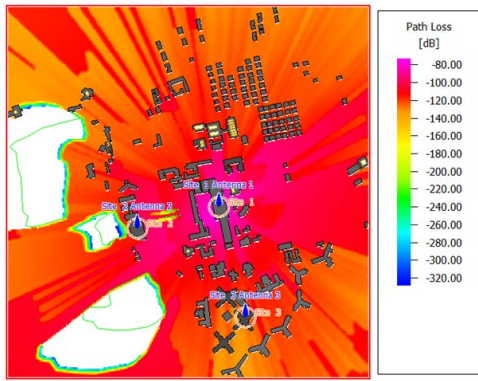
FIGURE 18. Simulation results of path loss over the selected geographical terrain for cell site 1.
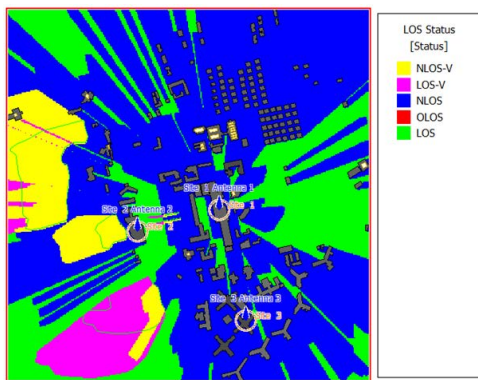

FIGURE 19. Layout of the geographical terrain with LOS and NLOS for cell site 1.

FIGURE 20. General transmitter and receiver scenario in knife edge diffraction model.

(a)

(b)

FIGURE 21. Analysis of different MIMO configurations with KED model (a) Data rate (b) Throughput.

and receiver the computational demand is ambitious. There are also even some scenarios where there is no 3D vector data available but only the clutter height information of the located building heights in pixel format. Kinfe edge diffraction(KED) model is one approach where the both cases can be predicted based on either vector or pixel data. This model considers the effect of the actual environment by utilizing the 3D vector building data along with terrain profile [24].

For the selected geographical terrain KED model is applied and the computation is done by using WinProp software. The number of diffractions (knife edges) can be limited to required number by editing the parameters in additional knife edge diffraction settings. The diffractions at the clutter objects including the clutter height are taken in to consideration for simulation. The general scenario how the knife edges are considered between transmitter and receiver during computation is shown below in Fig. 20. The simulations are carried out with unit cell MIMO antenna element, 2×2, 4×4 and 8×8 massive MIMO configuration radiation patterns. The effect of single stream data rate and throughput over the area of coverage as the number of antenna elements increases are observed shown in Fig. 21 (a) and (b).

The observed simulation results by implementing KED model are tabulated in Table 4. The single stream data rate
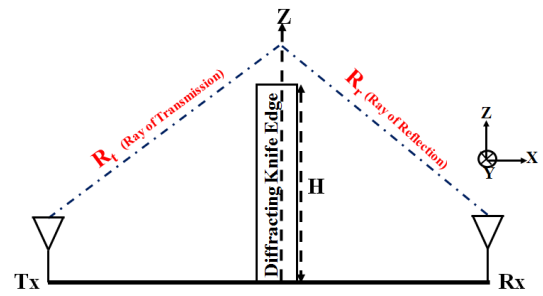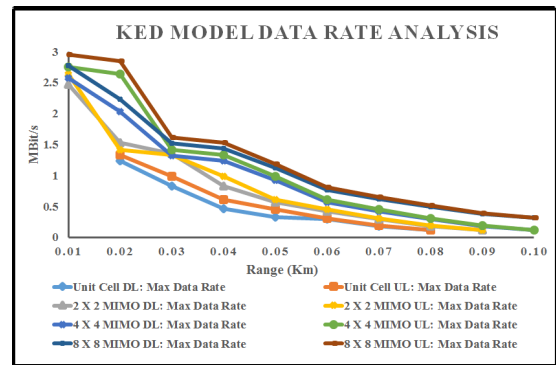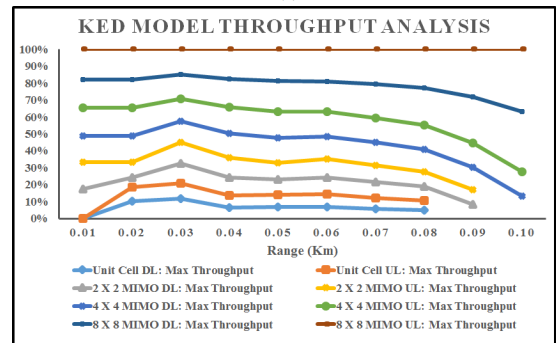
and throughput of 2.7764 MBits/s and 719.8 MBits/s for downlink and 2.956 MBits/s and 766.5 MBits/s for uplink are reported for the deployed cell sites at three locations A, B an C. From the simulation results RSRP is -85 dBm, RSRQ is 0 dB and RSSI is -62 dBm which states that the signal strength is excellent covering the entire map with selected locations A,B and C.

B. EXTENDED WALFISCH-IKEGAMI MODEL

Extended walfisch-ikegami model(EWM) considers several parameters related to building profile in the environment for path loss prediction. It utilizes very less computation time with tolerable accuracy when compared to the deterministic ray optical models. Wave-guiding effects are not considered

TABLE 4. Simulation results of various parameters with knife edge diffraction model.

S.No	Parameters	Sim.Res.	Exp.Val.
1.	DL:Max Data Rate (MBits/s)	2.776	—
2.	DL:Throughput (MBits/s)	719.8	—
3.	UL:Max Data Rate (MBits/s)	2.956	—
4.	UL:Throughput (MBits/s)	766.5	—
5.	SNIR (dB)	40 (E)	≥ 20
6.	RSRP (dBm)	-85 (E)	$\geq$ -80
7.	RSRQ (dB)	0 (E)	$\geq$ -10
8.	RSSI (dBm)	-62 (E)	$\geq$ -65

Note: E represents Excellent signal strength with maximum data speeds as per 3GPP.(Sim.Res.- Simulation Results; Exp.Val.-Expected Value)

in this model which generally occurs in urban canyons. This model accuracy is more accurate when the transmitters are located above the rooftop levels of the buildings as it approximates the multiple diffractions. It considers only the characteristic values for predicting path loss. It discriminates between line-of-sight (LOS) and non-line-of-sight(NLOS) situations.

The general propagation scenario of the EWM model is shown in Fig. 22. Where H_{Tx} is the height of the transmitter, H_{roof} is the mean value of the building heights, H_{Rx} is the height of the receiver, w is mean value of width of roads, s is mean value of building separation. The evaluation of path loss agress very well with the measurements of the base station antenna heights above the rooftop level. In this model the prediction error becomes quite larger for H_{Tx} close to H_{roof} when it is compared with the situations where $H_{Tx} >> H_{roof}$. The performance of this model is considered to be poor when $H_{Tx} << H_{roof}$ [24].
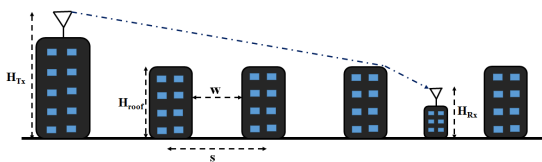

FIGURE 22. Propagation scenario with transmitter and receiver in extended walfisch-ikegami model.

For micro cells the prediction error is large and it does not consider the multipath propagation as a result wave guiding effects are not taken into account in computation. So, in situations where the transmitters are on over the rooftops this model provides good results. The single stream data rate and throughput for different MIMO antenna configurations over the considered geographical terrain with EWM are shown in Fig. 23 (a) and (b).

Using EWM model the simualtion results for the selected locations A,B and C deployed for this map are tabulated in Table 5. The data rates and throughput of 2.576 MBits/s and 669.8 MBits/s for downlink and 2.756 MBits/s and
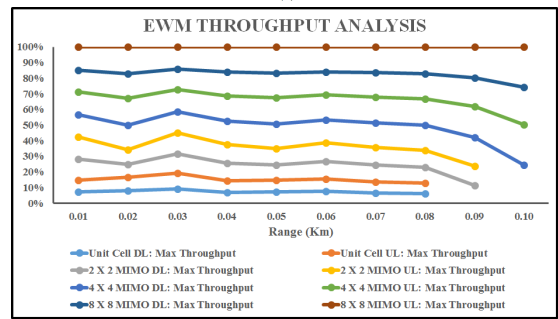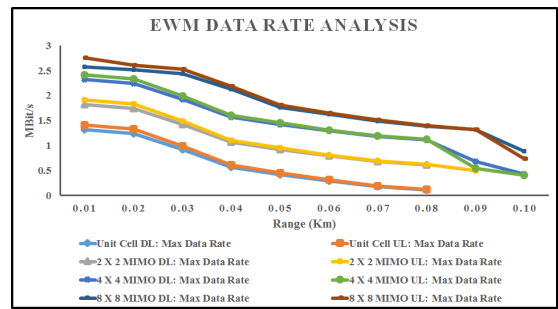

FIGURE 23. Analysis of different MIMO configurations with EWM (a) Data rate (b) Throughput.

TABLE 5. Simulation results of various parameters with extended Walfisch-ikegami model.

S.No	Parameters	Sim.Res.	Exp.Val.
1.	DL:Max Data Rate (MBits/s)	2.576	—
2.	DL:Throughput (MBits/s)	669.8	—
3.	UL:Max Data Rate (MBits/s)	2.756	—
4.	UL:Throughput (MBits/s)	716.5	—
5.	SNIR (dB)	40 (E)	≥ 20
6.	RSRP (dBm)	-80 (E)	$\geq$ -80
7.	RSRQ (dB)	0 (E)	$\geq$ -10
8.	RSSI (dBm)	-60 (E)	$\geq$ -65

Note: E represents Excellent signal strength with maximum data speeds as per 3GPP.(Sim.Res.- Simulation Results; Exp.Val.-Expected Value)

716.5 MBits/s for uplink are reported for the deployed cell sites. From the simulation results RSRP is -80 dBm, RSRQ is 0 dB and RSSI is -60 dBm which shows that the signal strength is good covering the entire map with deployed locations A,B and C.

C. DOMINANT PATH MODEL

Dominant path model(DPM) uses the full 3D approach in path searching and hence the results are more realistic and accurate. So far discussed wave propagation models are based on empirical approaches and they compute by direct ray between tranmitter and receiver location which often leads to erroneous results. This model determines the one dominant path between each transmitter and receiver pixel. The computation time is very less when compared to ray-tracing

models and accuracy is identical to knife edge diffraction model. As the ray tracing models are very time consuming and also they rely on vector database which indirectly influence the accuracy of prediction DPM are preferable. DPM determines the most siginificant one propagation path between transmitter and receiver which contributes to more than 90% of the total energy. This leads to less computation time and accuracy almost equivalent to ray-tracing models [26].

Ray tracing models (Knife edge diffraction) determine the numerous paths between transmitter and receiver, in empirical models (Extended Walfisch-ikegami Model) it considers the direct path but in DPM model it determines the most significant dominant path which requires less computation times. DPM model does not require preprocessing for vector database so it is ideal approach to compute coverage predictions in large urban areas. The computation path loss is given by using the following equation [24].

$$L = 20log(4\pi/\lambda) + 10plog(l) + \sum_{i=0}^{n} f(\phi, i) + \Omega + g_t \quad (1)$$

where L is the path loss computed for the receiver location, l is the distance between tranmitter and receiver, p is path loss component, f losses due to diffraction, g_t gain of transmitting antenna. The simulations are carried out with unit cell MIMO antenna element, 2×2, 4×4 MIMO and 8×8 massive MIMO configurations. The single stream data rate and throughput for different MIMO antenna configurations over the considered geographical terrain with DPM are shown in Fig. 24.
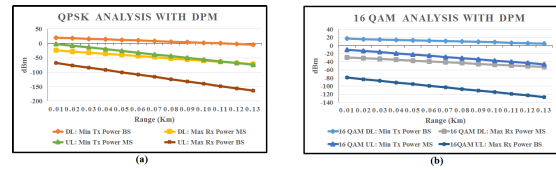

FIGURE 24. Analysis of different MIMO configurations with dominant path model (a) Data rate (b) Throughput.

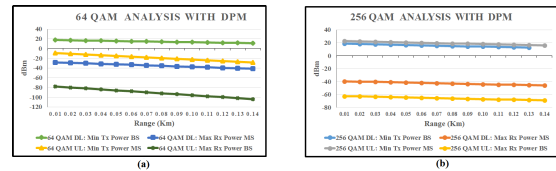**FIGURE 25.** (a) QPSK (b) 16 QAM analysis with dominant path model.

FIGURE 26. (a) 64 QAM (b) 256 QAM analysis with dominant path model.
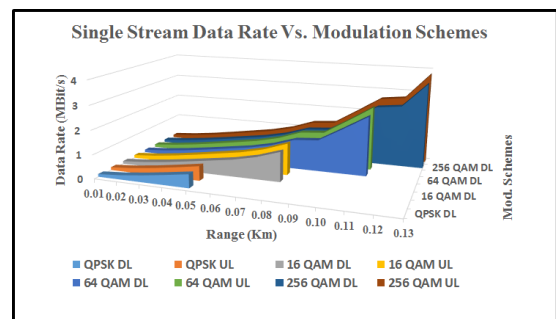

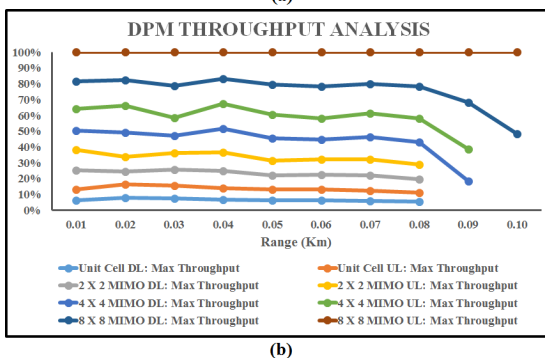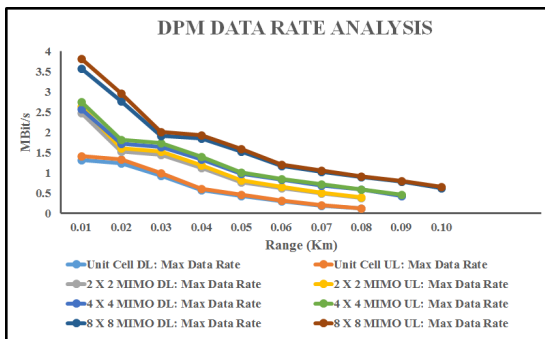**FIGURE 27.** Single stream data rate for different modulation schemes with dominant path model.

The detailed analysis with minimum transmitting and receiving power of base station(BS), mobile station(MS) for both down link (DL) and uplink (UL) are analysed with QPSK, 16 QAM, 64 QAM and 256 QAM modulation schemes are shown in Fig. 25 and 26. From the simulation results it is observed with 256 QAM for deployed base station at different locations A,B and C the maximum data rate and throughput are obtained. The comparison between the different modulation schemes with single stream of data for dominant path model are shown in Fig. 27.

By considering the 5G FDD wireless standard and dominant path wave propagation model the bandwidth is varied and observed the single stream of data for both downlink and uplink as shownin Fig. 28. From the simulation results it is observed with rise in bandwidth the data rate also increased. The maximum data rate of 1.37 GBit/s is reported with 20 MHz bandwidth for 8×8 massive MIMO by utilizing 64 dual polarized antenna elements both at the transmitter and receiver when compared with other MIMO configurations as shown in Fig. 29.

DPM simulation results for the deployed cell sites in the selected geographical terrain are tabluated in Table 6. The single stream data rate and throughput for both downlink and uplink are given in Fig. 30. The data rates and throughput of 3.577 MBits/s and 930.1 MBits/s for downlink and
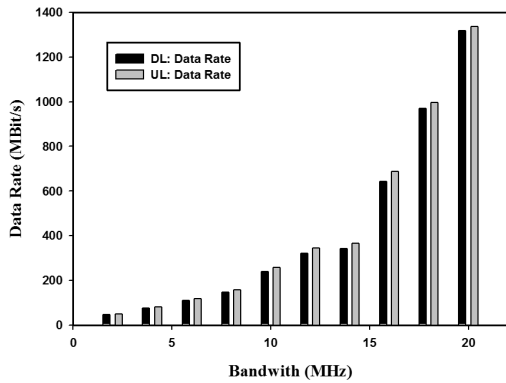
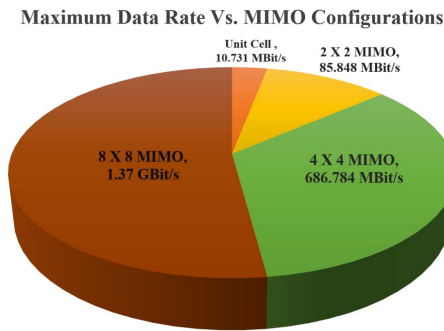**FIGURE 28.** Data rate and bandwidth variation with dominant path model.

FIGURE 29. Maximum data rate with different MIMO configurations for dominant path model with same number of antennas at both transmitter and receiver.

TABLE 6. Simulation results of various parameters with dominant path model.

S.No	Parameters	Sim.Res.	Exp.Val.
1.	DL:Max Data Rate (MBits/s)	3.577	—
2.	DL:Throughput (MBits/s)	930.1	—
3.	UL:Max Data Rate (MBits/s)	3.827	—
4.	UL:Throughput (MBits/s)	995.0	—
5.	SNIR (dB)	60 (E)	≥ 20
6.	RSRP (dBm)	-60 (E)	≥ -80
7.	RSRQ (dB)	0 (E)	≥ -10
8.	RSSI (dBm)	-40 (E)	≥ -65

Note: E represents Excellent signal strength with maximum data speeds as per 3GPP.(Sim.Res.- Simulation Results; Exp.Val.- Expected Value)

3.827 MBits/s and 995.0 MBits/s for uplink are reported for the deployed cell sites. The SNIR is simulated as 60 dB for 8 × 8 massive MIMO configuration and given in Fig. 31(a). The signal strength and quality parameters RSRQ, RSRP and RSSI are shown in Fig. 31(b), Fig. 32(a) and 32(b) respectively. From the simulation results RSRP is -60 dBm, RSRQ
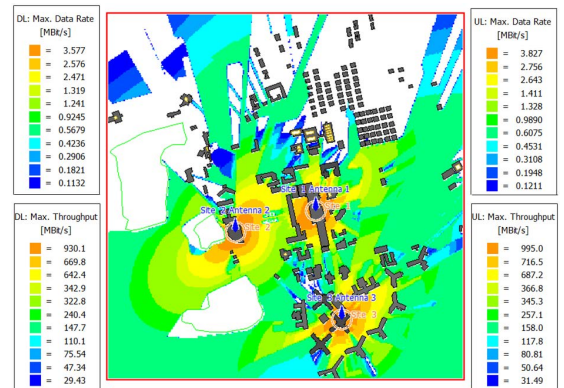

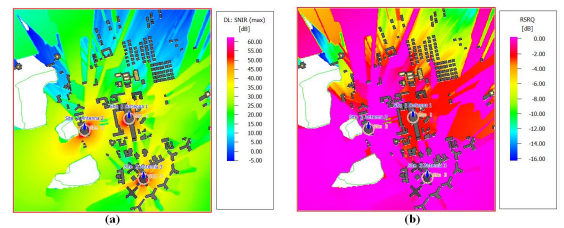**FIGURE 30.** Data rate and throughput of downlink and uplink with dominant path model for 8 × 8 massive MIMO.

FIGURE 31. (a) Received power and SNIR (b) RSRQ for the map area with dominant path model.
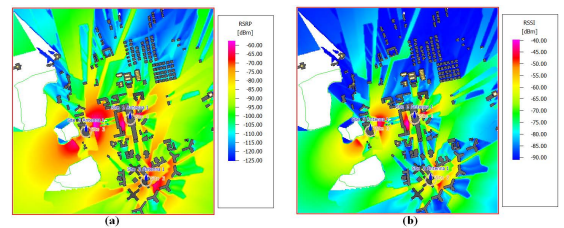

FIGURE 32. (a) RSRP (b) RSSI for the layout with dominant path model.

is 0 dB and RSSI is -40 dBm which shows that the signal strength is excellent covering the entire map with selected locations of base stations at A,B and C.

V. CONCLUSION

Dual polarized printed multiple input multiple output (MIMO) antenna for Band 42 (3.4 - 3.6 GHz) with wave propagation models is presented. An isolation of 32 dB between the two ports and an average gain of 8.26 dB for each polarized antenna element is measured. The designed dual polarized antenna element, 2 × 2, 4 × 4 and 8 × 8 massive MIMO antenna configuration radiation patterns are deployed in selected geographical situation for detailed radio network planning using FEKO WinProp platform. Dominant path model provides data rate and throughput of 3.827, 995 MBit/s and 3.577, 930.1 MBit/s for single stream of data in uplink and downlink respectively. By comparing all the three wave propagtion models dominant path model provides the maximum data rate of of 1.37 GBits/s with utmost signal quality

covering the entire geographical site by evaluating 256 QAM modulation technique with 8×8 massive MIMO antenna configuration.

REFERENCES

[1] H. Huang, Y. Liu, and S. Gong, "A broadband dual-polarized base station antenna with sturdy construction," *IEEE Antennas Wireless Propag. Lett.*, vol. 16, pp. 665–668, 2017, doi: 10.1109/LAWP.2016.2598181.

[2] G. Cui, S.-G. Zhou, G. Zhao, and S.-X. Gong, "A compact dual-band dual-polarized antenna for base station application," *Prog. Electromagn. Res. C*, vol. 64, pp. 61–70, 2016.

[3] Y. Cheng, Y. Li, and W. Lu, "A novel compact dual-polarized antenna," *Int. J. Antennas Propag.*, vol. 2016, pp. 1–5, Jan. 2016, doi: 10.1155/2016/6304356.

[4] H. Huang, X. Li, and Y. Liu, "A low-profile, dual-polarized patch antenna for 5G MIMO application," *IEEE Trans. Antennas Propag.*, vol. 67, no. 2, pp. 1275–1279, Feb. 2019, doi: 10.1109/TAP.2018.2880098.

[5] K.-B. Kim, B. C. Jung, and J.-M. Woo, "A compact dual-polarized (CP, LP) with dual-feed microstrip patch array for target detection," *IEEE Antennas Wireless Propag. Lett.*, vol. 19, no. 4, pp. 517–521, Apr. 2020, doi: 10.1109/LAWP.2019.2961159.

[6] X. Qin and Y. Li, "Compact dual-polarized cross-slot antenna with colocated feeding," *IEEE Trans. Antennas Propag.*, vol. 67, no. 11, pp. 7139–7143, Nov. 2019, doi: 10.1109/TAP.2019.2936758.

[7] L.-H. Wen, S. Gao, Q. Luo, C.-X. Mao, W. Hu, Y. Yin, Y. Zhou, and Q. Wang, "Compact dual-polarized shared-dipole antennas for base station applications," *IEEE Trans. Antennas Propag.*, vol. 66, no. 12, pp. 6826–6834, Dec. 2018, doi: 10.1109/TAP.2018.2871717.

[8] Q. Zhang and Y. Gao, "A compact broadband dual-polarized antenna array for base stations," *IEEE Antennas Wireless Propag. Lett.*, vol. 17, no. 6, pp. 1073–1076, Jun. 2018, doi: 10.1109/LAWP.2018.2832293.

[9] Y. Cui, X. Gao, H. Fu, Q.-X. Chu, and R. Li, "Broadband dual-polarized dual-dipole planar antennas: Analysis, design, and application for base stations," *IEEE Antennas Propag. Mag.*, vol. 59, no. 6, pp. 77–87, Dec. 2017, doi: 10.1109/MAP.2017.2753038.

[10] D.-L. Wen, D.-Z. Dong, and Q.-X. Chu, "A wideband differentially fed dual-polarized antenna with stable radiation pattern for base stations," *IEEE Trans. Antennas Propag.*, vol. 65, no. 5, pp. 2248–2255, May 2017, doi: 10.1109/TAP.2017.2679762.

[11] Z.-Y. Zhang and K.-L. Wu, "A wideband dual-polarized dielectric magneto-electric dipole antenna," *IEEE Trans. Antennas Propag.*, vol. 66, no. 10, pp. 5590–5595, Oct. 2018, doi: 10.1109/TAP.2018.2859914.

[12] M. Li, X. Chen, A. Zhang, and A. A. Kishk, "Dual-polarized broadband base station antenna backed with dielectric cavity for 5G communications," *IEEE Antennas Wireless Propag. Lett.*, vol. 18, no. 10, pp. 2051–2055, Oct. 2019, doi: 10.1109/LAWP.2019.2937201.

[13] B. Yin, S. Zhao, P. Wang, and X. Feng, "Isolation improvement of compact microbase station antenna based on metasurface spatial filtering," *IEEE Trans. Electromagn. Compat.*, vol. 63, no. 1, pp. 57–65, Feb. 2021, doi: 10.1109/TEMC.2020.3004189.

[14] C. H. Le Thi, S. X. Ta, X. Q. Nguyen, K. K. Nguyen, and C. Dao-Ngoc, "Design of compact broadband dual-polarized antenna for 5G applications," *Int. J. RF Microw. Comput.-Aided Eng.*, vol. 31, no. 5, May 2021, Art. no. e22615, doi: 10.1002/mmce.22615.

[15] B. Anudeep, K. Krishnamoorthy, and P. H. Rao, "Low-profile, wideband dual-polarized 1×2 MIMO antenna with FSS decoupling technique," *Int. J. Microw. Wireless Technol.*, pp. 1–7, May 2021, doi: 10.1017/S1759078721000805.

[16] Y. Aslan, J. Puskely, A. Roederer, and A. Yarovoy, "Performance comparison of single- and multi-lobe antenna arrays in 5G urban outdoor environments at mm-waves via intelligent ray tracing," in *Proc. 14th Eur. Conf. Antennas Propag. (EuCAP)*, Mar. 2020, pp. 1–5, doi: 10.23919/EuCAP48036.2020.9135263.

[17] G. Gampala and C. J. Reddy, "Massive MIMO—Beyond 4G and A basis for 5G," in *Proc. Int. Appl. Comput. Electromagn. Soc. Symp. (ACES)*, Mar. 2018, pp. 1–2, doi: 10.23919/ROPACES.2018.8364192.

[18] B. B. Haile, E. Mutafungwa, and J. Hamalainen, "A data-driven multiobjective optimization framework for hyperdense 5G network planning," *IEEE Access*, vol. 8, pp. 169423–169443, 2020, doi: 10.1109/ACCESS.2020.3023452.

[19] *3rd Generation Partnership Project*. Accessed: Oct. 2021. [Online]. Available: http://www.3gpp.org/news-events

[20] R. Hoppe, G. Wolfle, P. Futter, and J. Soler, "Wave propagation models for 5G radio coverage and channel analysis," in *Proc. 6th Asia–Pacific Conf. Antennas Propag. (APCAP)*, Oct. 2017, pp. 1–3, doi: 10.1109/APCAP.2017.8420499.

[21] D. Pinchera, M. D. Migliore, and F. Schettino, "Optimizing antenna arrays for spatial multiplexing: Towards 6G systems," *IEEE Access*, vol. 9, pp. 53276–53291, 2021, doi: 10.1109/ACCESS.2021.3070198.

[22] M. Stefanovic, S. R. Panic, R. A. A. de Souza, and J. Reig, "Recent advances in RF propagation modeling for 5G systems," *Int. J. Antennas Propag.*, vol. 2017, pp. 1–5, Jan. 2017, doi: 10.1155/2017/4701208.

[23] T. S. Rappaport, Y. Xing, G. R. MacCartney, A. F. Molisch, E. Mellios, and J. Zhang, "Overview of millimeter wave communications for fifth-generation (5G) wireless networks—With a focus on propagation models," *IEEE Trans. Antennas Propag.*, vol. 65, no. 12, pp. 6213–6230, Dec. 2017, doi: 10.1109/TAP.2017.2734243.

[24] WinProp. *Wave Propagation and Radio Network Planning Software (Part of Altair HyperWorks)*. Accessed: Aug. 23, 2021. [Online]. Available: https://www.altair.com/

[25] WinProp. *A New Dimension of Wave Propagation and Radio Network Planning*. Accessed: Apr. 7, 2020. [Online]. Available: https://altairhyperworks.com/product/feko/winprop-propagationmodeling

[26] FEKO. *Comprehensive Electromagnetic Analysis Software Suite (Part of Altair HyperWorks)*. Accessed: Aug. 23, 2021. [Online]. Available: https://www.altair.com/

ANUDEEP BELLARY (Student Member, IEEE) received the B.Tech. degree in electronics and communication engineering from JNTUA, Andhra Pradesh, India, in 2013, and the M.Tech. degree in communication engineering from VIT University, Tamil Nadu, India, in 2015. He is currently pursuing the Ph.D. degree in electronics and communication with the National Institute of Technology Karnataka, Surathkal, Mangalore, India. His research interests include antennas, multi-in multi-out (MIMO) antennas, mutual coupling, and metamaterials.

KRISHNAMOORTHY KANDASAMY (Member, IEEE) received the B.E. degree in electronics and communication engineering from Bharathiar University, Coimbatore, India, in 2003, the M.E. degree in communication systems from the College of Engineering, Guindy, Anna University, Chennai, India, in 2007, and the Ph.D. degree in electrical engineering from the IIT Bombay, Mumbai, India, in 2016. He is currently an Assistant Professor with the Department of Electronics and Communication Engineering, National Institute of Technology Karnataka, Surathkal, India. His current research interests include metamaterials, antenna engineering, microwave integrated circuits (MICs), and monolithic MICs.

PATNAM HANUMANTHA RAO (Senior Member, IEEE) received the B.Tech. degree from Sri Venkateswara University, Tirupati, India, the M.S. degree from the Birla Institute of Technology and Science, Pilani, India, and the Ph.D. degree from the Queen's University of Belfast, Belfast, U.K. He was with the Space Applications Center, Indian Space Research Organization, Ahmedabad, India, for a period of two years. After that, he joined the SAMEER-Center for Electromagnetics, Chennai, India. He has more than 30 years of research experience in antennas and electromagnetics. In 2010, he steered a computational electromagnetic cell, a joint collaborative project by IISc-SAMEER to analyze complex electromagnetic problems, such as antennas on ship, satellite, and aircraft. He has authored over 100 papers in journals and conferences and presented papers in various national and international conferences. His current research interests include antenna designs for multi-in multi-out (MIMO), massive MIMO, and switched beam antenna arrays for 5G communications applications.

• • •